[12] G. Bresler, D. Cartwright, and D. Tse, "Setting the feasibility of interference alignment for the MIMO interference channel: The SYMMETRIC SQUARE case," arXiv:1104.0888, Apr. 2011.
[13] M. Razaviyayn, G. Lyubeznik, and Z.-Q. Luo, "On the degrees of freedom achievable through interference alignment in a MIMO interference channel," *IEEE Trans. Signal Process.*, vol. 60, no. 2, pp. 812–821, Feb. 2012.
[14] O. E. Ayach, S. W. Peters, and R. W. Heath, "The feasibility of interference alignment over measured MIMO-OFDM channels," *IEEE Trans. Veh. Technol.*, vol. 59, no. 9, pp. 4309–4321, Nov. 2010.
[15] H. Park, S.-H. Park, J.-S. Kim, and I. Lee, "SINR balancing techniques in coordinated multi-cell downlink systems," *IEEE Trans. Wireless Commun.*, vol. 12, no. 2, pp. 626–635, Feb. 2013.
[16] K. Gomadam, V. R. Cadambe, and S. A. Jafar, "A distributed numerical approach to interference alignment and applications to wireless interference networks," *IEEE Trans. Inf. Theory*, vol. 57, no. 6, pp. 3309–3322, Jun. 2011.

MSE-Based Hybrid RF/Baseband Processing for Millimeter-Wave Communication Systems in MIMO Interference Channels

Minhyun Kim, *Student Member, IEEE*, and
Yong H. Lee, *Senior Member, IEEE*

***Abstract*—We consider the design of a hybrid multiple-input multiple-output (MIMO) processor consisting of a radio frequency (RF) beamformer and a baseband MIMO processor for millimeter-wave communications over multiuser interference channels. Sparse approximation problems are formulated to design hybrid MIMO processors approximating the minimum-mean-square-error transmit/receive processors in MIMO interference channels. They are solved by orthogonal-matching-pursuit-based algorithms that successively select RF beamforming vectors from a set of candidate vectors and optimize the corresponding baseband processor in the least squares sense. It is shown that various beamformers can be designed by considering different types of candidate vector sets. Simulation results demonstrate the advantage of the proposed design over the conventional method that designs the baseband processor after steering the RF beams.**

***Index Terms*—Hybrid radio frequency (RF)/baseband processing, mean square error criterion, millimeter-wave (mm-wave) communication, multiple-input multiple-output (MIMO) interference channel, orthogonal matching pursuit (OMP), sparse approximation.**

I. Introduction

Due to its vast unlicensed bandwidth, millimeter-wave (mm-wave) communication has been receiving considerable attention as a potential technique for future wireless communications [1], [2]. By employing large antenna arrays that can be built in a small volume due to the short wavelength, mm-wave systems can overcome high path loss experienced in their channels. Unfortunately, however, the high cost for implementing radio frequency (RF) chains consisting of amplifiers, mixers, and analog-to-digital/digital-to-analog converters in a mm-wave band prevents the system from allocating a dedicated RF chain for each antenna. As a result, mm-wave systems usually employ a hybrid multiple-input multiple-output (MIMO) processor consisting of an analog beamformer in RF band and a digital MIMO processor in baseband. The RF beamformer in such a system reduces the required number of RF chains by precoding/combining of antenna signals.

Hybrid MIMO processors have been proposed for single-user MIMO systems both in the current microwave communications [3]–[5] and in the mm-wave communications [6]–[9]. An RF beamformer whose coefficients are realized by phase shifters, which is called a *phased array* beamformer, was designed by extracting the phases of singular vectors of the MIMO channel matrix [3]. A subarray-based RF receive beamformer maximizing the system capacity was proposed [4], and a minimum mean square error (MMSE) technique for jointly designing the RF beamformer and the baseband MIMO processor was developed [5]. In particular, Venkateswaran and van der Veen in [5] proposed an MMSE-based matching pursuit algorithm to choose the coefficients of RF beamformers from a set of all complex coefficients with finite precision. In [6], transmit/receive (Tx/Rx) RF beamformers were jointly designed by maximizing a capacity lower bound. Recently, in [7]–[9], the authors developed a joint design technique for the hybrid MIMO processor based on the orthogonal matching pursuit (OMP) method, which is popular for sparse approximation [10], where RF beamforming vectors are selected from the set of array response vectors pointing the angle of arrivals/departures (AoAs/AoDs).

In this paper, we consider mm-wave systems over multiuser interference channels and develop an OMP-based algorithm to design hybrid MIMO processors that approximate the optimal MMSE Tx/Rx processors for MIMO interference channels [11], [12]. The hybrid processor for the receiver is designed by extending the hybrid MMSE receivers in [5] and [9], and the hybrid Tx processor is designed based on the equivalent system that models the *reverse* of the interference channel. The OMP algorithm successively selects RF beamforming vectors from a set of candidate vectors using the MMSE criterion and optimizes the corresponding baseband processor in the least squares sense. It is shown that various beamformers with different performances and complexity characteristics can be designed by considering different types of candidate sets including the set of eigenvectors and discrete Fourier transform (DFT) vectors.

Notations: Throughout this paper, we use boldface uppercase letters to denote matrices and boldface lowercase letters for column vectors. Superscript $(\cdot)^H$ denotes conjugate transpose. $\|\mathbf{A}\|_F$, $\|\mathbf{A}\|_0$, and $\mathrm{rank}(\mathbf{A})$ are the Frobenius norm, the ℓ_0 norm, and the rank of matrix $\mathbf{A}$, respectively. $\mathrm{diag}(\mathbf{A})$ is a vector consisting of diagonal elements of $\mathbf{A}$, and $\mathrm{diag}(\mathbf{A}, \mathbf{B})$ is a block diagonal matrix with $\mathbf{A}$ and $\mathbf{B}$ on the diagonal blocks. $(\mathbf{A})_{i,j}$ is the (i, j)th entry of $\mathbf{A}$, $\mathbf{a}(l)$ is its lth column vector, and $\mathcal{C}(\mathbf{A})$ is the column space of $\mathbf{A}$. $[\mathbf{A}|\mathbf{B}]$ denotes horizontal concatenation, and $\mathbb{E}[\cdot]$ is the expectation operator. The $N \times N$ identity matrix is denoted by $\mathbf{I}_N$.

II. System and Channel Models

A. System Model

We consider a K-user MIMO interference channel where each user's terminal is equipped with a hybrid MIMO processor (see Fig. 1). The transmitters have N_t antennas and N_t^RF RF chains. The receivers have N_r antennas and N_r^RF chains, and each user sends N_s data streams. Here $N_\mathrm{t}^\mathrm{RF} < N_\mathrm{t}$, $N_\mathrm{r}^\mathrm{RF} < N_\mathrm{r}$, and N_s is chosen to meet both $N_\mathrm{s} \leq \min(N_\mathrm{t}^\mathrm{RF}, N_\mathrm{r}^\mathrm{RF})$ and the feasibility of the degrees of freedom

Manuscript received November 29, 2013; revised April 28, 2014 and July 24, 2014; accepted July 26, 2014. Date of publication August 8, 2014; date of current version June 16, 2015. This work was supported in part by the ICT R&D program of the MSIP/IITP [14-000-04-001, Development of Radio Access Technologies for 5G Mobile Communications]. The review of this paper was coordinated by Dr. S. Tomasin.

The authors are with the Department of Electrical Engineering, Korea Advanced Institute of Science and Technology (KAIST), Daejeon 305-701, Korea (e-mail: mhkim@stein.kaist.ac.kr; yohlee@kaist.ac.kr).

Color versions of one or more of the figures in this paper are available online at http://ieeexplore.ieee.org.
Digital Object Identifier 10.1109/TVT.2014.2346400

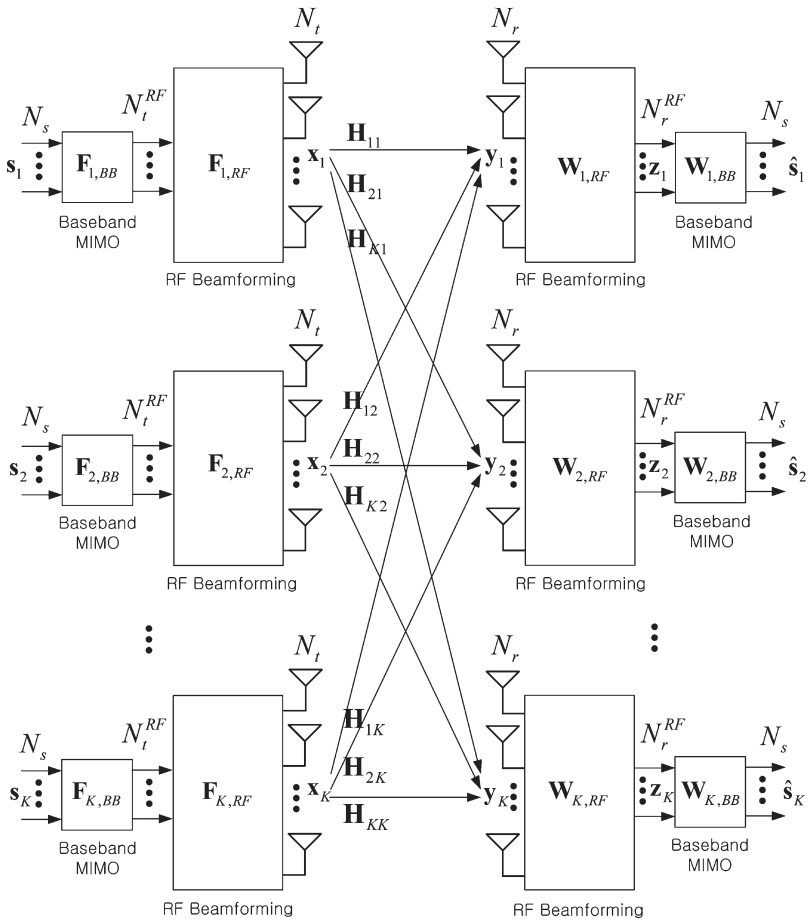

Fig. 1. A K-user MIMO interference channel where each terminal is equipped with a hybrid MIMO processor.

in MIMO interference networks [13].[1] The hybrid MIMO processor of the kth transmitter consists of the $N_{\mathrm{t}}^{\mathrm{RF}} \times N_{\mathrm{s}}$ baseband precoder, i.e., $\mathbf{F}_{k,\mathrm{BB}}$, followed by the $N_{\mathrm{t}} \times N_{\mathrm{t}}^{\mathrm{RF}}$ RF beamformer, i.e., $\mathbf{F}_{k,\mathrm{RF}}$, and that of the corresponding receiver consists of the $N_{\mathrm{r}} \times N_{\mathrm{r}}^{\mathrm{RF}}$ RF beamformer, i.e., $\mathbf{W}_{k,\mathrm{RF}}$, followed by the $N_{\mathrm{r}}^{\mathrm{RF}} \times N_{\mathrm{s}}$ baseband combiner, i.e., $\mathbf{W}_{k,\mathrm{BB}}$. We assume a narrowband block-fading propagation channel and denote the $N_{\mathrm{r}} \times N_{\mathrm{t}}$ channel matrix from the jth sender to the kth receiver by $\mathbf{H}_{kj}$. Using these notations, the transmitted signal from the kth sender is written as $\mathbf{x}_k = \mathbf{F}_{k,\mathrm{RF}}\mathbf{F}_{k,\mathrm{BB}}\mathbf{s}_k$, where $\mathbf{s}_k \in \mathbb{C}^{N_{\mathrm{s}} \times 1}$ is a vector of complex information symbols to be transmitted. It is assumed that each stream of $\mathbf{s}_k$ is encoded from the Gaussian codebook, i.e., $\mathbf{s}_k \sim \mathcal{CN}(0, \mathbf{I}_{N_{\mathrm{s}}})$, and $\|\mathbf{F}_{k,\mathrm{RF}}\mathbf{F}_{k,\mathrm{BB}}\|_F^2 \leq P_k$, where P_k is the transmit power of the kth sender. The received signal at the kth receiver is given by

$$\mathbf{y}_k = \mathbf{H}_{kk}\mathbf{F}_{k,\mathrm{RF}}\mathbf{F}_{k,\mathrm{BB}}\mathbf{s}_k + \sum_{j \neq k}^{K} \mathbf{H}_{kj}\mathbf{F}_{j,\mathrm{RF}}\mathbf{F}_{j,\mathrm{BB}}\mathbf{s}_j + \mathbf{n}_k \quad (1)$$

where $\mathbf{n}_k \in \mathbb{C}^{N_{\mathrm{r}} \times 1}$ is additive white Gaussian noise (AWGN) with $\mathbf{n}_k \sim \mathcal{CN}(0, \sigma^2 \mathbf{I}_{N_{\mathrm{r}}})$. The received signal $\mathbf{y}_k$ is passed through the RF beamformer, i.e., $\mathbf{W}_{k,\mathrm{RF}}$, and the baseband MIMO processor, i.e., $\mathbf{W}_{k,\mathrm{BB}}$. The output of the baseband processor, i.e., $\hat{\mathbf{s}}_k$, is written as

$$\hat{\mathbf{s}}_k = \mathbf{W}_{k,\mathrm{BB}}^H \mathbf{z}_k \quad (2)$$

$$= \mathbf{W}_{k,\mathrm{BB}}^H \mathbf{W}_{k,\mathrm{RF}}^H \mathbf{H}_{kk}\mathbf{F}_{k,\mathrm{RF}}\mathbf{F}_{k,\mathrm{BB}}\mathbf{s}_k \quad (3)$$

$$+ \mathbf{W}_{k,\mathrm{BB}}^H \mathbf{W}_{k,\mathrm{RF}}^H \sum_{j \neq k}^{K} \mathbf{H}_{kj}\mathbf{F}_{j,\mathrm{RF}}\mathbf{F}_{j,\mathrm{BB}}\mathbf{s}_j$$

$$+ \mathbf{W}_{k,\mathrm{BB}}^H \mathbf{W}_{k,\mathrm{RF}}^H \mathbf{n}_k \quad (4)$$

where $\mathbf{z}_k = \mathbf{W}_{k,\mathrm{RF}}^H \mathbf{y}_k$ is the beamformer output.

B. Channel Model

We adopt the parametric channel model in [9], which is based on the extended Saleh–Valenzuela model [14] that has been used for modeling a 60-GHz wireless local area network [15] and personal area network [16]. The channel matrix $\mathbf{H}_{kj}$ is represented as

$$\mathbf{H}_{kj} = \sqrt{\frac{N_{\mathrm{t}} N_{\mathrm{r}}}{N_{\mathrm{cl}} N_{\mathrm{ray}}}} \sum_{m=1}^{N_{\mathrm{cl}}} \sum_{n=1}^{N_{\mathrm{ray}}} \alpha_{mn}^{(kj)} \times \mathbf{a}_{\mathrm{r}}\left(\phi_{mn}^{\mathrm{r}(k)}, \theta_{mn}^{\mathrm{r}(k)}\right) \mathbf{a}_{\mathrm{t}}\left(\phi_{mn}^{\mathrm{t}(j)}, \theta_{mn}^{\mathrm{t}(j)}\right)^H \quad (5)$$

where N_{cl} is the number of scattering clusters, N_{ray} is the number of rays per cluster, and $\alpha_{mn}^{(kj)}$ is the complex gain of the nth ray in the mth cluster. $\phi_{mn}^{\mathrm{r}}(\theta_{mn}^{\mathrm{r}})$ and $\phi_{mn}^{\mathrm{t}}(\theta_{mn}^{\mathrm{t}})$ are the azimuth (elevation)

[1] Assuming that the coefficients of the effective channel, i.e., $\mathbf{W}_{k,\mathrm{RF}}^H \mathbf{H}_{kj}\mathbf{F}_{j,\mathrm{RF}}$, are drawn independent and identically distributed from a continuous distribution, the feasibility condition is stated as follows [13]: $N_{\mathrm{s}} \leq \min(N_{\mathrm{t}}^{\mathrm{RF}}, N_{\mathrm{r}}^{\mathrm{RF}})$ when $K \leq R$, and $N_{\mathrm{s}} \leq (R/(R+1)) \min(N_{\mathrm{t}}^{\mathrm{RF}}, N_{\mathrm{r}}^{\mathrm{RF}})$, otherwise, where $R = \lfloor \max(N_{\mathrm{t}}^{\mathrm{RF}}, N_{\mathrm{r}}^{\mathrm{RF}}) / \min(N_{\mathrm{t}}^{\mathrm{RF}}, N_{\mathrm{r}}^{\mathrm{RF}}) \rfloor$.

AoA and AoD, respectively. The gains $\{\alpha_{mn}^{(kj)}\}$ are complex Gaussian random variables with zero mean and variance σ_α^2. The mean angle associated with each cluster is uniformly distributed over $[-\pi, \pi)$, and the distribution of the difference between an AoA (AoD) and its mean is Laplacian with angular standard deviation $\sigma_{\rm AS}$ [14]. The vectors $\mathbf{a}_{\rm r}(\phi_{mn}^{\rm r}, \theta_{mn}^{\rm r})$ and $\mathbf{a}_{\rm t}(\phi_{mn}^{\rm t}, \theta_{mn}^{\rm t})$ are the array response vectors at the receiver and the transmitter, respectively.

III. Hybrid MIMO Processor Design

Here, we first review the mean square error (MSE)-based processors in [11] and [12] and then derive the proposed hybrid processors for the receiver and the transmitter. We assume that all channel information is perfectly available at all terminals.

A. MSE-Based Interference Suppression

For a conventional MIMO system where each antenna is connected to a separate RF chain (full-complexity RF chains), an $N_{\rm t} \times N_{\rm s}$ precoder $\mathbf{F}_k$ and an $N_{\rm r} \times N_{\rm s}$ combiner $\mathbf{W}_k$ are employed in place of $\mathbf{F}_{k,\rm RF}\mathbf{F}_{k,\rm BB}$ and $\mathbf{W}_{k,\rm RF}\mathbf{W}_{k,\rm BB}$ in Fig. 1, respectively. An MSE-based optimization problem for designing the precoder and the combiner is written as

$$\min_{\{\mathbf{F}_k\},\{\mathbf{W}_k\}} \quad \sum_{k=1}^{K} \mathbb{E}\left\|\mathbf{s}_k - \hat{\mathbf{s}}_k\right\|^2 \quad \text{s.t.} \quad \|\mathbf{F}_k\|_F^2 \le P_k,\ k \in \{1,\ldots,K\}. \tag{6}$$

Since the total MSE function is not jointly convex over the precoding and combining matrices, $\{\mathbf{F}_k\}(\{\mathbf{W}_k\})$ is optimized while fixing $\{\mathbf{W}_k\}(\{\mathbf{F}_k\})$. The optimal solutions are given by

$$\mathbf{W}_k^{\rm o} = \left(\sum_{i=1}^{K} \mathbf{H}_{ki}\mathbf{F}_i\mathbf{F}_i^H\mathbf{H}_{ki}^H + \sigma^2\mathbf{I}_{N_{\rm r}}\right)^{-1}\mathbf{H}_{kk}\mathbf{F}_k \tag{7}$$

$$\mathbf{F}_k^{\rm o} = \left(\sum_{i=1}^{K} \mathbf{H}_{ik}^H\mathbf{W}_i\mathbf{W}_i^H\mathbf{H}_{ik} + \lambda_k\mathbf{I}_{N_{\rm t}}\right)^{-1}\mathbf{H}_{kk}^H\mathbf{W}_k \tag{8}$$

where $\lambda_k \ge 0$ is the Lagrangian multiplier that is numerically obtained to meet the power constraint [11], [12]. In (7), the terms inside the parenthesis form a nonsingular matrix, and thus, the realization of the Rx processor, i.e., $\mathbf{W}_k^{\rm o}$, is straightforward. On the other hand, in (8), such nonsingularity is not always guaranteed if $\lambda_k = 0$. This is particularly problematic in mm-wave communications where $KN_{\rm s} < \min(N_{\rm t}, N_{\rm r})$. For such systems with large antenna arrays, $\sum_{i=1}^{K}\mathbf{H}_{ik}^H\mathbf{W}_i\mathbf{W}_i^H\mathbf{H}_{ik}$ in (8) becomes singular because $\mathrm{rank}(\sum_{i=1}^{K}\mathbf{H}_{ik}^H\mathbf{W}_i\mathbf{W}_i^H\mathbf{H}_{ik}) \le KN_{\rm s}$. To avoid this problem, we assume that $\lambda_k \ge \varepsilon$ for all k, where ε is a small positive number.[2]

The MMSE solutions in (7) and (8) are iteratively obtained. At each iteration, $\mathbf{W}_k^{\rm o}$ is evaluated for a given $\mathbf{F}_k^{\rm o}$, and then, $\mathbf{F}_k^{\rm o}$ is updated using the newly obtained $\mathbf{W}_k^{\rm o}$. The iteration continues until a stopping criterion is satisfied. The hybrid MIMO processors presented below approximate the resulting MMSE processors.

B. Design of Rx Hybrid MIMO Systems

The proposed hybrid processor is derived by decomposing $\mathbf{W}_k^{\rm o}$ in (7) into the product of $\mathbf{W}_{k,\rm RF}^{\rm o}$ and $\mathbf{W}_{k,\rm BB}^{\rm o}$. The MMSE solution in (7) can be rewritten as

$$\mathbf{W}_k^{\rm o} = \mathbf{R}_{\mathbf{y}_k}^{-1}\mathbf{R}_{\mathbf{y}_k\mathbf{s}_k} \tag{9}$$

where $\mathbf{R}_{\mathbf{y}_k} = \mathbb{E}[\mathbf{y}_k\mathbf{y}_k^H]$ and $\mathbf{R}_{\mathbf{y}_k\mathbf{s}_k} = \mathbb{E}[\mathbf{y}_k\mathbf{s}_k^H]$. Similarly, if $\mathbf{W}_{k,\rm RF}$ is given, the optimal baseband processing matrix, i.e., $\mathbf{W}_{k,\rm BB}^{\rm o}$, is written as

$$\mathbf{W}_{k,\rm BB}^{\rm o} = \mathbf{R}_{\mathbf{z}_k}^{-1}\mathbf{R}_{\mathbf{z}_k\mathbf{s}_k} = \left(\mathbf{W}_{k,\rm RF}^H\mathbf{R}_{\mathbf{y}_k}\mathbf{W}_{k,\rm RF}\right)^{-1}\mathbf{W}_{k,\rm RF}^H\mathbf{R}_{\mathbf{y}_k\mathbf{s}_k} \tag{10}$$

where $\mathbf{R}_{\mathbf{z}_k} = \mathbb{E}[\mathbf{z}_k\mathbf{z}_k^H]$ and $\mathbf{R}_{\mathbf{z}_k\mathbf{s}_k} = \mathbb{E}[\mathbf{z}_k\mathbf{s}_k^H]$. Since (10) holds for any $\mathbf{W}_{k,\rm RF}$, the problem for designing the MMSE hybrid processor, i.e., $(\mathbf{W}_{k,\rm RF}^{\rm o}, \mathbf{W}_{k,\rm BB}^{\rm o})$, reduces to

$$\mathbf{W}_{k,\rm RF}^{\rm o} = \arg\min_{\mathbf{W}_{k,\rm RF}} \mathbb{E}\left\|\mathbf{s}_k - \left(\mathbf{W}_{k,\rm BB}^{\rm o}\right)^H\mathbf{W}_{k,\rm RF}^H\mathbf{y}_k\right\|^2 \tag{11}$$

where $\mathbf{W}_{k,\rm BB}^{\rm o}$ is given by (10). This problem can be rephrased as in the following lemma.

Lemma 1: The MMSE beamformer in (11) can be obtained by solving

$$\mathbf{W}_{k,\rm RF}^{\rm o} = \arg\min_{\mathbf{W}_{k,\rm RF}} \left\|\mathbf{R}_{\mathbf{y}_k}^{\frac{1}{2}}\mathbf{W}_k^{\rm o} - \mathbf{R}_{\mathbf{y}_k}^{\frac{1}{2}}\mathbf{W}_{k,\rm RF}\mathbf{W}_{k,\rm BB}^{\rm o}\right\|_F^2 \tag{12}$$

where $\mathbf{W}_k^{\rm o}$ and $\mathbf{W}_{k,\rm BB}^{\rm o}$ are given by (9) and (10), respectively.

This lemma can be proved by extending either the proof in [5], which assumes transmitters with a single antenna, or the proof in [9], which considers single-user MIMO systems. Such an extension is rather straightforward, and thus, the proof is omitted. Following the approach in [9], we design $\mathbf{W}_{k,\rm RF}$ by choosing appropriate vectors from a set of candidate beamformers, which is denoted as $\mathcal{S}_{\rm W-BF}$, based on (12). In (12), the columns of $\mathbf{R}_{\mathbf{y}_k}^{1/2}\mathbf{W}_k^{\rm o}$ and those of $\mathbf{R}_{\mathbf{y}_k}^{1/2}\mathbf{W}_{k,\rm RF}$ are located in $\mathcal{C}(\mathbf{R}_{\mathbf{y}_k}^{1/2})$, and the former is approximated by linear combinations of the latter. This fact suggests that the columns of $\mathbf{R}_{\mathbf{y}_k}^{1/2}\mathbf{W}_{k,\rm RF}$ be selected from the basis of $\mathcal{C}(\mathbf{R}_{\mathbf{y}_k}^{1/2})$. Next, we present six kinds of $\mathcal{S}_{\rm W-BF}$'s whose elements premultiplied with $\mathbf{R}_{\mathbf{y}_k}^{1/2}$ can form the bases of $\mathcal{C}(\mathbf{R}_{\mathbf{y}_k}^{1/2})$. These sets lead to various beamformers with different performances and complexity characteristics.

- Eigenbeamformer: $\mathcal{S}_{\rm W-BF}$ consists of the eigenvectors of $\mathbf{R}_{\mathbf{y}_k}$. The Frobenius norm in (12) can be represented as $\sum_{i=1}^{N_{\rm s}}\left\|\mathbf{R}_{\mathbf{y}_k}^{1/2}\mathbf{w}_k^{\rm o}(i) - \mathbf{R}_{\mathbf{y}_k}^{1/2}\mathbf{W}_{k,\rm RF}\mathbf{w}_{k,\rm BB}^{\rm o}(i)\right\|^2$ for the ith columns of $\mathbf{W}_k^{\rm o}$ and $\mathbf{W}_{k,\rm BB}^{\rm o}$. This sum of squared errors is minimized if we choose the $N_{\rm r}^{\rm RF}$ dominant eigenvectors of $\mathbf{R}_{\mathbf{y}_k}^{1/2}$ (or equivalently $\mathbf{R}_{\mathbf{y}_k}$) and use them for RF beamforming. This beamformer requires both gain controllers and phase shifters in the RF domain for implementation. It is more complex to implement than the other beamformers described below.
- Array response beamformer: To reduce the complexity of the RF circuits, we may consider the use of phased array beamformers, which can be implemented using phase shifters. One candidate $\mathcal{S}_{\rm W-BF}$ for such beamforming is the set of array response vectors pointing the AoAs of the desired user [9]. The array response vectors are linearly independent with probability 1 when $N_{\rm cl}N_{\rm ray} \le \min(N_{\rm t}, N_{\rm r})$.
- DFT beamformer: Another type of phased array beamformers can be designed by using the columns of $N_{\rm r} \times N_{\rm r}$ DFT matrix as the elements of $\mathcal{S}_{\rm W-BF}$.

[2] An alternative to this heuristic approach is to consider the modified MSE criterion, which has been used for designing MIMO Tx filters [17]. The extension of such MMSE filters to the MMSE problem under consideration requires further work that is out of the scope of this paper.

- Discrete cosine transform (DCT) beamformer: Use of the columns of $N_{\rm r} \times N_{\rm r}$ DCT matrix for $\mathcal{S}_{\rm W-BF}$ results in a beamformer with real-valued coefficients that can be realized using gain controllers and 1-bit phase shifters.
- Discrete Hadamard transform (DHT) beamformer: To further simplify the implementation, at the expense of performance degradation, DHT may be employed instead of DCT/DFT. Use of DHT yields a binary-valued beamformer that can be realized using 1-bit phase shifters. This beamformer can be considerably simpler to implement than the beamformers previously mentioned.
- Antenna selection: An MMSE-based antenna selection scheme can be derived by choosing $\mathcal{S}_{\rm W-BF}$ consisting of the columns of $\mathbf{I}_{N_{\rm r}}$. This is the simplest beamformer that can be realized using a switching circuit.

The performances of these six types of beamformers will be compared through computer simulation in Section IV.

Before proceeding further, we present an interesting property of eigenbeamformers indicating that eigenbeamforming enables perfect decomposition of $\mathbf{W}_k^{\rm o}$ into $\mathbf{W}_{k,{\rm RF}}^{\rm o}\mathbf{W}_{k,{\rm BB}}^{\rm o}$ in (12). To show this property, we need the following notations: $\mathbf{R}_{\mathbf{y}_k} = \mathbf{U}\mathbf{\Lambda}\mathbf{U}^H$, where $\mathbf{\Lambda}$ is a diagonal matrix consisting of eigenvalues of $\mathbf{R}_{\mathbf{y}_k}$, which are arranged in decreasing order, and $\mathbf{U}$ is the corresponding eigenvector matrix. The matrix $\mathbf{U}$ is decomposed as $\mathbf{U} = [\mathbf{U}_1, \mathbf{U}_2]$, where $\mathbf{U}_1$ consists of the $N_{\rm r}^{\rm RF}$ dominant eigenvectors, and $\mathbf{U}_2$ consists of the rest. Similarly, $\mathbf{\Lambda}$ is decomposed as $\mathbf{\Lambda} = {\rm diag}(\mathbf{\Lambda}_1, \mathbf{\Lambda}_2)$, where $\mathbf{\Lambda}_i$ $(i = 1, 2)$ correspond to $\mathbf{U}_i$. Next, we present a lemma that is useful for deriving the desired property.

Lemma 2: If $N_{\rm r}^{\rm RF} \geq KN_{\rm s} \geq r$, then $\mathbf{U}_2^H\mathbf{R}_{\mathbf{y}_k\mathbf{s}_k} = \mathbf{0}$, where $r = {\rm rank}(\sum_{i=1}^K \mathbf{H}_{ki}\mathbf{F}_i\mathbf{F}_i^H\mathbf{H}_{ki}^H)$, and $\mathbf{0}$ is a matrix whose entries are all zeros.

Proof: From (1), $\mathbf{R}_{\mathbf{y}_k} = \sum_{i=1}^K \mathbf{H}_{ki}\mathbf{F}_i\mathbf{F}_i^H\mathbf{H}_{ki}^H + \sigma^2\mathbf{I}_{N_{\rm r}}$. Thus, r eigenvalues of $\mathbf{R}_{\mathbf{y}_k}$ are greater than σ^2, and the rest is equal to σ^2. Since $\mathbf{\Lambda} = \mathbf{U}^H\mathbf{R}_{\mathbf{y}_k}\mathbf{U} = {\rm diag}(\mathbf{U}_1^H\mathbf{R}_{\mathbf{y}_k}\mathbf{U}_1, \mathbf{U}_2^H\mathbf{R}_{\mathbf{y}_k}\mathbf{U}_2)$, then $\mathbf{U}_2^H\mathbf{R}_{\mathbf{y}_k}\mathbf{U}_2 = \sum_{i=1}^K \mathbf{U}_2^H\mathbf{H}_{ki}\mathbf{F}_i\mathbf{F}_i^H\mathbf{H}_{ki}^H\mathbf{U}_2 + \sigma^2\mathbf{I}_{N_{\rm r}-N_{\rm r}^{\rm RF}} = \sigma^2\mathbf{I}_{N_{\rm r}-N_{\rm r}^{\rm RF}}$. From the last equality, we obtain $\sum_{i=1}^K \mathbf{U}_2^H\mathbf{H}_{ki}\mathbf{F}_i\mathbf{F}_i^H\mathbf{H}_{ki}^H\mathbf{U}_2 = \mathbf{0}$, which leads to $\mathbf{U}_2^H\mathbf{H}_{kk}\mathbf{F}_k\mathbf{F}_k^H\mathbf{H}_{kk}^H\mathbf{U}_2 = \mathbf{0}$ because $\mathbf{U}_2^H\mathbf{H}_{ki}\mathbf{F}_i\mathbf{F}_i^H\mathbf{H}_{ki}^H\mathbf{U}_2$ is positive semidefinite for all i. Hence, $\mathbf{U}_2^H\mathbf{H}_{kk}\mathbf{F}_k = \mathbf{U}_2^H\mathbf{R}_{\mathbf{y}_k\mathbf{s}_k} = \mathbf{0}$. This completes the proof. ■

Using *Lemma 2*, we develop the following property.

Property 1: Suppose that the eigenbeamformer consisting of the $N_{\rm r}^{\rm RF}$ dominant eigenvectors is employed $\mathbf{W}_{k,{\rm RF}}^{\rm o} = \mathbf{U}_1$ and $N_{\rm r}^{\rm RF} \geq KN_{\rm s} \geq r$. Then, the Frobenius norm in (12) corresponding to the optimal $\mathbf{W}_{k,{\rm RF}}^{\rm o}$ reduces to zero, i.e., $\mathbf{W}_k^{\rm o} = \mathbf{W}_{k,{\rm RF}}^{\rm o}\mathbf{W}_{k,{\rm BB}}^{\rm o}$.

Proof: From (9), $\mathbf{W}_k^{\rm o} = \mathbf{U}\mathbf{\Lambda}^{-1}\mathbf{U}^H\mathbf{R}_{\mathbf{y}_k\mathbf{s}_k} = \mathbf{U}_1\mathbf{\Lambda}_1^{-1}\mathbf{U}_1^H\mathbf{R}_{\mathbf{y}_k\mathbf{s}_k} = \mathbf{W}_{k,{\rm RF}}^{\rm o}\mathbf{\Lambda}_1^{-1}\mathbf{U}_1^H\mathbf{R}_{\mathbf{y}_k\mathbf{s}_k}$, where the second equality holds due to *Lemma 2*. Thus, it is sufficient to prove that $\mathbf{W}_{k,{\rm BB}}^{\rm o} = \mathbf{\Lambda}_1^{-1}\mathbf{U}_1^H\mathbf{R}_{\mathbf{y}_k\mathbf{s}_k}$. Indeed, from (10), $\mathbf{W}_{k,{\rm BB}}^{\rm o} = (\mathbf{U}_1^H\mathbf{R}_{\mathbf{y}_k}\mathbf{U}_1)^{-1}\mathbf{U}_1^H\mathbf{R}_{\mathbf{y}_k\mathbf{s}_k} = \mathbf{\Lambda}_1^{-1}\mathbf{U}_1^H\mathbf{R}_{\mathbf{y}_k\mathbf{s}_k}$. This completes the proof. ■

Property 1 indicates that in K-user interference channels, $N_{\rm r}^{\rm RF}$ should be determined depending on both K and $N_{\rm s}$.

Suppose that the set $\mathcal{S}_{\rm W-BF}$ is given. The RF beamformer is designed by solving a sparse approximation problem based on (12). To formulate the problem, we first form an $N_{\rm r} \times N_{\rm b}$ matrix $\mathbf{B}_{\mathbf{y}_k}$ whose columns consist of the elements of $\mathcal{S}_{\rm W-BF}$ as its columns ($N_{\rm b}$ is the number of elements in $\mathcal{S}_{\rm W-BF}$) and then rewrite the error matrix $\mathbf{R}_{\mathbf{y}_k}^{1/2}\mathbf{W}_k^{\rm o} - \mathbf{R}_{\mathbf{y}_k}^{1/2}\mathbf{W}_{k,{\rm RF}}\mathbf{W}_{k,{\rm BB}}^{\rm o}$ in (12) as $\mathbf{R}_{\mathbf{y}_k}^{1/2}\mathbf{W}_k^{\rm o} - \mathbf{R}_{\mathbf{y}_k}^{1/2}\mathbf{B}_{\mathbf{y}_k}\widetilde{\mathbf{W}}_{k,{\rm BB}}^{\rm o}$, where $\widetilde{\mathbf{W}}_{k,{\rm BB}}^{\rm o}$ is an $N_{\rm b} \times N_{\rm s}$ matrix having $N_{\rm r}^{\rm RF}$ nonzero rows that constitute $\mathbf{W}_{k,{\rm BB}}^{\rm o}$ (columns of $\widetilde{\mathbf{W}}_{k,{\rm BB}}^{\rm o}$ are $N_{\rm r}^{\rm RF}$-sparse vectors). The positions of the nonzero rows correspond to the selected columns of $\mathbf{B}_{\mathbf{y}_k}$: The ith row of $\widetilde{\mathbf{W}}_{k,{\rm BB}}^{\rm o}$ is nonzero if the ith column of $\mathbf{B}_{\mathbf{y}_k}$ is chosen for RF beamforming. The sparse approximation problem is written as

$$\widetilde{\mathbf{W}}_{k,{\rm BB}}^{\rm o} = \underset{\widetilde{\mathbf{W}}_{k,{\rm BB}}}{\arg\min} \left\| \mathbf{R}_{\mathbf{y}_k}^{\frac{1}{2}}\mathbf{W}_k^{\rm o} - \mathbf{R}_{\mathbf{y}_k}^{\frac{1}{2}}\mathbf{B}_{\mathbf{y}_k}\widetilde{\mathbf{W}}_{k,{\rm BB}} \right\|_F^2 \quad \text{s.t.} \quad \left\| {\rm diag}\left(\widetilde{\mathbf{W}}_{k,{\rm BB}}\widetilde{\mathbf{W}}_{k,{\rm BB}}^H\right) \right\|_0 = N_{\rm r}^{\rm RF}. \tag{13}$$

In (13), the columns of $\mathbf{R}_{\mathbf{y}_k}^{1/2}\mathbf{W}_k^{\rm o}$ are approximated by the linear combination of the columns of $\mathbf{R}_{\mathbf{y}_k}^{1/2}\mathbf{B}_{\mathbf{y}_k}$, where the weights for the linear combination are given by the nonzero elements of $\widetilde{\mathbf{W}}_{k,{\rm BB}}^{\rm o}$. Using the sparse approximation framework, an OMP algorithm [10] for jointly designing the RF beamforming matrix $\mathbf{W}_{k,{\rm RF}}$ and the corresponding baseband MIMO processor $\mathbf{W}_{k,{\rm BB}}$ can be summarized as in Algorithm 1. At each iteration, the column of $\mathbf{R}_{\mathbf{y}_k}^{1/2}\mathbf{B}_{\mathbf{y}_k}$ that is most strongly correlated with the residual $\mathbf{R}_{\mathbf{y}_k}^{1/2}\mathbf{W}_{k,{\rm res}}$ is chosen (steps 4 and 5). Then, the selected column, which is denoted as $\mathbf{b}_{\mathbf{y}_k}(l)$, is appended to $\mathbf{W}_{k,{\rm RF}}$ (step 6); $\mathbf{W}_{k,{\rm BB}}$ is obtained by solving the least squares problem $\mathbf{R}_{\mathbf{y}_k}^{1/2}\mathbf{W}_k^{\rm o} \approx \mathbf{R}_{\mathbf{y}_k}^{1/2}\mathbf{W}_{k,{\rm RF}}\mathbf{W}_{k,{\rm BB}}$ (step 7); and the residual $\mathbf{W}_{k,{\rm res}}$ is updated by subtracting the contribution of the selected RF beamforming vector to $\mathbf{W}_k^{\rm o}$ (step 8).

Algorithm 1 OMP-based Rx hybrid MIMO processor

Require: $\{\mathbf{W}_k^{\rm o}\}$
1: $\mathbf{W}_{k,{\rm RF}} =$ Empty Matrix
2: $\mathbf{W}_{k,{\rm res}} = \mathbf{W}_k^{\rm o}$
3: **for** $i \leq N_{\rm r}^{\rm RF}$ **do**
4: $\quad\mathbf{\Psi}_k = \left(\mathbf{R}_{\mathbf{y}_k}^{1/2}\mathbf{B}_{\mathbf{y}_k}\right)^H\left(\mathbf{R}_{\mathbf{y}_k}^{1/2}\mathbf{W}_{k,{\rm res}}\right)$
5: $\quad l = \arg\max_{m=1,\ldots,N_{\rm b}}(\mathbf{\Psi}_k\mathbf{\Psi}_k^H)_{m,m}$
6: $\quad\mathbf{W}_{k,{\rm RF}} = [\mathbf{W}_{k,{\rm RF}}|\mathbf{b}_{\mathbf{y}_k}(l)]$
7: $\quad\mathbf{W}_{k,{\rm BB}} = \left(\mathbf{W}_{k,{\rm RF}}^H\mathbf{R}_{\mathbf{y}_k}\mathbf{W}_{k,{\rm RF}}\right)^{-1}\mathbf{W}_{k,{\rm RF}}^H\mathbf{R}_{\mathbf{y}_k}\mathbf{W}_k^{\rm o}$
8: $\quad\mathbf{W}_{k,{\rm res}} = (\mathbf{W}_k^{\rm o} - \mathbf{W}_{k,{\rm RF}}\mathbf{W}_{k,{\rm BB}})/\|\mathbf{W}_k^{\rm o} - \mathbf{W}_{k,{\rm RF}}\mathbf{W}_{k,{\rm BB}}\|_F$
9: **end for**
10: **return** $\mathbf{W}_{k,{\rm RF}}$, $\mathbf{W}_{k,{\rm BB}}$

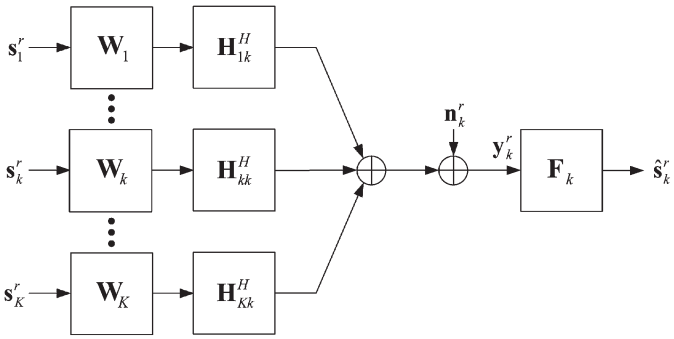

Fig. 2. Equivalent system that models the reverse of the interference channel in Fig. 1, where $\{\mathbf{s}_k^{\rm r}\}$ are $N_{\rm s} \times 1$ Tx vectors of the reverse system, and $\mathbf{n}_k^{\rm r}$ is an $N_{\rm t} \times 1$ AWGN vector with $\mathbf{n}_k^{\rm r} \sim \mathcal{CN}(0, \lambda_k\mathbf{I}_{N_{\rm t}})$.

C. Design of Tx Hybrid MIMO Systems

The hybrid processor at the transmitter is designed based on the equivalent system, shown in Fig. 2, that models the reverse of the interference channel in Fig. 1. The reverse system is defined so that the optimal Tx filter of the forward system in (8) can be obtained from the optimal Rx filter of the reverse system. Note that the right-hand side of (8) can be obtained from that of (7) by replacing $\{\mathbf{F}_i\}$ with $\{\mathbf{W}_i\}$,

$\{\mathbf{H}_{ki}\}$ with $\{\mathbf{H}_{ik}^H\}$, and σ^2 with λ_k. Thus, the reverse system in Fig. 2 employs $\{\mathbf{W}_k\}$ and $\{\mathbf{F}_k\}$ as its Tx and Rx filters, respectively, and models the interference channel from the jth transmitter to the kth receiver using $\{\mathbf{H}_{jk}^H\}$ for $j \neq k$. In addition, the noise variance when using this system is assumed to be λ_k $(\mathbf{n}_k^{\mathrm{r}} \sim \mathcal{CN}(0, \lambda_k \mathbf{I}_{N_{\mathrm{t}}}))$. The input/output relation of the reverse system is given by

$$\hat{\mathbf{s}}_k^{\mathrm{r}} = \mathbf{F}_k^H \left(\mathbf{H}_{kk}^H \mathbf{W}_k \mathbf{s}_k^{\mathrm{r}} + \sum_{j \neq k} \mathbf{H}_{jk}^H \mathbf{W}_j \mathbf{s}_j^{\mathrm{r}} + \mathbf{n}_k^{\mathrm{r}} \right) \triangleq \mathbf{F}_k^H \mathbf{y}_k^{\mathrm{r}} \quad (14)$$

where $\mathbf{y}_k^{\mathrm{r}} = \mathbf{H}_{kk}^H \mathbf{W}_k \mathbf{s}_k^{\mathrm{r}} + \sum_{j \neq k} \mathbf{H}_{jk}^H \mathbf{W}_j \mathbf{s}_j^{\mathrm{r}} + \mathbf{n}_k^{\mathrm{r}}$. Due to the definition of the reverse system, the optimal Rx filter of the reverse system minimizing $\sum_{k=1}^K \mathbb{E}\|\mathbf{s}_k^{\mathrm{r}} - \hat{\mathbf{s}}_k^{\mathrm{r}}\|^2$ is given by (8). Now, we decompose $\mathbf{F}_k^{\mathrm{o}}$ into the product $\mathbf{F}_{k,\mathrm{RF}}^{\mathrm{o}} \mathbf{F}_{k,\mathrm{BB}}^{\mathrm{o}}$ at the receiver side of the reverse system. By adopting the process for obtaining $\mathbf{W}_{k,\mathrm{RF}}^{\mathrm{o}}$ in (12), we have the following lemma.

Lemma 3: The MMSE beamformer $\mathbf{F}_{k,\mathrm{RF}}^{\mathrm{o}}$ can be obtained by solving

$$\mathbf{F}_{k,\mathrm{RF}}^{\mathrm{o}} \arg\min_{\mathbf{F}_{k,\mathrm{RF}}} \left\| \mathbf{R}_{\mathbf{y}_k^{\mathrm{r}}}^{\frac{1}{2}} \mathbf{F}_k^{\mathrm{o}} - \mathbf{R}_{\mathbf{y}_k^{\mathrm{r}}}^{\frac{1}{2}} \mathbf{F}_{k,\mathrm{RF}} \mathbf{F}_{k,\mathrm{BB}}^{\mathrm{o}} \right\|_F^2 \quad (15)$$

where $\mathbf{F}_{k,\mathrm{BB}}^{\mathrm{o}} = (\mathbf{F}_{k,\mathrm{RF}}^H \mathbf{R}_{\mathbf{y}_k^{\mathrm{r}}} \mathbf{F}_{k,\mathrm{RF}})^{-1} \mathbf{F}_{k,\mathrm{RF}}^H \mathbf{R}_{\mathbf{y}_k^{\mathrm{r}} \mathbf{s}_k^{\mathrm{r}}}$ for $\mathbf{R}_{\mathbf{y}_k^{\mathrm{r}} \mathbf{s}_k^{\mathrm{r}}} = \mathbb{E}[\mathbf{y}_k^{\mathrm{r}} \mathbf{s}_k^{\mathrm{r}\,H}]$, $\mathbf{R}_{\mathbf{y}_k^{\mathrm{r}}} = \mathbb{E}[\mathbf{y}_k^{\mathrm{r}} \mathbf{y}_k^{\mathrm{r}\,H}]$, and $\mathbf{F}_k^{\mathrm{o}}$ is given by (8).

This lemma can be proved as in *Lemma 1*. As before, we design $\mathbf{F}_{k,\mathrm{RF}}$ by choosing appropriate vectors from a set of candidate beamformers, which is denoted as $\mathcal{S}_{\mathrm{F-BF}}$ in this case. Among the six types of beamformer sets considered for $\mathbf{W}_{k,\mathrm{RF}}$, those for the eigenbeamformer and the array response beamformer need slight modifications, whereas the rest remains the same. Specifically, $\mathcal{S}_{\mathrm{F-BF}}$ for eigenbeamforming consists of the eigenvectors of $\mathbf{R}_{\mathbf{y}_k^{\mathrm{r}}}$ and that for array response beamforming has the array response vectors pointing the AoAs of the desired user (or the AoDs of the original forward system). Due to the similarity between (12) and (15), the sparse approximation problem can also be formulated as before. We form an $N_{\mathrm{t}} \times N_{\mathrm{b}}$ matrix $\mathbf{B}_{\mathbf{y}_k^{\mathrm{r}}}$ consisting of the elements of $\mathcal{S}_{\mathrm{F-BF}}$ and then rewrite the error matrix $\mathbf{R}_{\mathbf{y}_k^{\mathrm{r}}}^{1/2} \mathbf{F}_k^{\mathrm{o}} - \mathbf{R}_{\mathbf{y}_k^{\mathrm{r}}}^{1/2} \mathbf{F}_{k,\mathrm{RF}} \mathbf{F}_{k,\mathrm{BB}}^{\mathrm{o}}$ in (15) as $\mathbf{R}_{\mathbf{y}_k^{\mathrm{r}}}^{1/2} \mathbf{F}_k^{\mathrm{o}} - \mathbf{R}_{\mathbf{y}_k^{\mathrm{r}}}^{1/2} \mathbf{B}_{\mathbf{y}_k^{\mathrm{r}}} \widetilde{\mathbf{F}}_{k,\mathrm{BB}}^{\mathrm{o}}$, where $\widetilde{\mathbf{F}}_{k,\mathrm{BB}}^{\mathrm{o}}$ is an $N_{\mathrm{b}} \times N_{\mathrm{s}}$ matrix having $N_{\mathrm{t}}^{\mathrm{RF}}$ nonzero rows that constitute $\mathbf{F}_{k,\mathrm{BB}}^{\mathrm{o}}$. The positions of the nonzero rows correspond to the selected columns of $\mathbf{B}_{\mathbf{y}_k^{\mathrm{r}}}$: The ith row of $\widetilde{\mathbf{F}}_{k,\mathrm{BB}}^{\mathrm{o}}$ is nonzero if the ith column of $\mathbf{B}_{\mathbf{y}_k^{\mathrm{r}}}$ is chosen for RF beamforming. The sparse approximation problem is written as

$$\begin{aligned} \widetilde{\mathbf{F}}_{k,\mathrm{BB}}^{\mathrm{o}} = \arg\min_{\widetilde{\mathbf{F}}_{k,\mathrm{BB}}} & \left\| \mathbf{R}_{\mathbf{y}_k^{\mathrm{r}}}^{\frac{1}{2}} \mathbf{F}_k^{\mathrm{o}} - \mathbf{R}_{\mathbf{y}_k^{\mathrm{r}}}^{\frac{1}{2}} \mathbf{B}_{\mathbf{y}_k^{\mathrm{r}}} \widetilde{\mathbf{F}}_{k,\mathrm{BB}} \right\|_F^2 \\ \text{s.t.} & \left\| \mathrm{diag}\left(\widetilde{\mathbf{F}}_{k,\mathrm{BB}} \widetilde{\mathbf{F}}_{k,\mathrm{BB}}^H \right) \right\|_0 = N_{\mathrm{t}}^{\mathrm{RF}} \\ \text{and} & \left\| \mathbf{B}_{\mathbf{y}_k^{\mathrm{r}}} \widetilde{\mathbf{F}}_{k,\mathrm{BB}} \right\|_F^2 = \|\mathbf{F}_k^{\mathrm{o}}\|_F^2 \end{aligned} \quad (16)$$

where the second constraint is added to keep the Tx power equal to that of $\mathbf{F}_k^{\mathrm{o}}$. The OMP algorithm for obtaining $\mathbf{F}_{k,\mathrm{RF}}^{\mathrm{o}}$ is summarized in Algorithm 2. In this algorithm, steps 1–9 correspond to those of Algorithm 1. One exception is step 10, which is added to realize the power constraint. The resulting filters, i.e., $(\mathbf{F}_{k,\mathrm{RF}}^{\mathrm{o}}, \mathbf{F}_{k,\mathrm{BB}}^{\mathrm{o}})$, are used for the Tx precoding in the original interference channel.

Algorithm 2 OMP-based Tx hybrid MIMO processor

Require: $\{\mathbf{F}_k^{\mathrm{o}}\}$
1: $\mathbf{F}_{k,\mathrm{RF}} =$ Empty Matrix
2: $\mathbf{F}_{k,\mathrm{res}} = \mathbf{F}_k^{\mathrm{o}}$
3: **for** $i \leq N_{\mathrm{t}}^{\mathrm{RF}}$ **do**
4: $\quad \mathbf{\Psi}_k = (\mathbf{R}_{\mathbf{y}_k^{\mathrm{r}}}^{1/2} \mathbf{B}_{\mathbf{y}_k^{\mathrm{r}}})^H (\mathbf{R}_{\mathbf{y}_k^{\mathrm{r}}}^{1/2} \mathbf{F}_{k,\mathrm{res}})$
5: $\quad l = \arg\max_{m=1,\ldots,N_{\mathrm{b}}} (\mathbf{\Psi}_k \mathbf{\Psi}_k^H)_{m,m}$
6: $\quad \mathbf{F}_{k,\mathrm{RF}} = [\mathbf{F}_{k,\mathrm{RF}} | \mathbf{b}_{\mathbf{y}_k^{\mathrm{r}}}(l)]$
7: $\quad \mathbf{F}_{k,\mathrm{BB}} = (\mathbf{F}_{k,\mathrm{RF}}^H \mathbf{R}_{\mathbf{y}_k^{\mathrm{r}}} \mathbf{F}_{k,\mathrm{RF}})^{-1} \mathbf{F}_{k,\mathrm{RF}}^H \mathbf{R}_{\mathbf{y}_k^{\mathrm{r}}} \mathbf{F}_k^{\mathrm{o}}$
8: $\quad \mathbf{F}_{k,\mathrm{res}} = (\mathbf{F}_k^{\mathrm{o}} - \mathbf{F}_{k,\mathrm{RF}} \mathbf{F}_{k,\mathrm{BB}}) / \|\mathbf{F}_k^{\mathrm{o}} - \mathbf{F}_{k,\mathrm{RF}} \mathbf{F}_{k,\mathrm{BB}}\|_F$
9: **end for**
10: $\mathbf{F}_{k,\mathrm{BB}} = \|\mathbf{F}_k^{\mathrm{o}}\|_F (\mathbf{F}_{k,\mathrm{BB}} / \|\mathbf{F}_{k,\mathrm{RF}} \mathbf{F}_{k,\mathrm{BB}}\|_F)$
11: **return** $\mathbf{F}_{k,\mathrm{RF}}$, $\mathbf{F}_{k,\mathrm{BB}}$

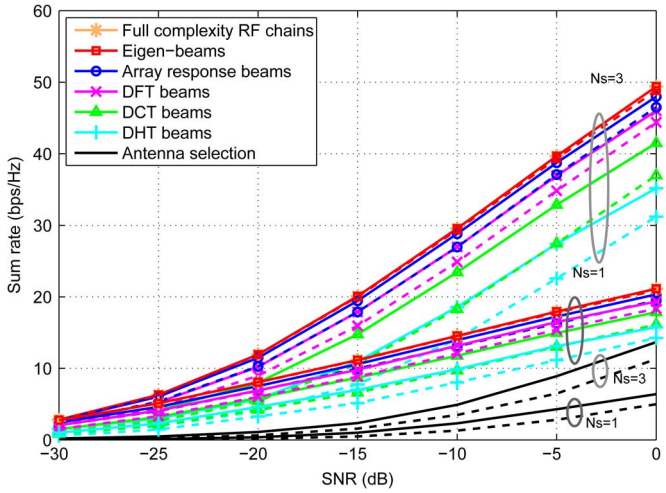

Fig. 3. Sum rate performance against SNR when $K = 2$, $N_{\mathrm{cl}} = 3$, and $N_{\mathrm{s}} \in \{1, 3\}$. Here, the solid and dotted curves correspond to the proposed OMP-based method and the beam-steering method, respectively.

IV. Simulation Results

The average sum rate performances of the proposed OMP-based methods are examined through computer simulation. For comparison, we also evaluate the sum rate performance of the optimal MMSE design in systems with full-complexity RF chains ($N_{\mathrm{t}}^{\mathrm{RF}} = N_{\mathrm{t}}, N_{\mathrm{r}}^{\mathrm{RF}} = N_{\mathrm{r}}$), which directly realize (7) and (8) in baseband, and the beam-steering methods that separately design the RF beamformer and the baseband MIMO processor. For the latter, the RF beams are selected from $\mathcal{S}_{\mathrm{W-BF}}/\mathcal{S}_{\mathrm{F-BF}}$ using the OMP algorithm as in the proposed methods; however, in this case, the Frobenius norms in (12) and (15) are evaluated without multiplying the square-root covariance matrices $(\mathbf{R}_{\mathbf{y}_k}^{1/2}, \mathbf{R}_{\mathbf{y}_k^{\mathrm{r}}}^{1/2})$. The baseband MIMO processors are designed by (7) and (8) for the effective channels obtained after setting the RF beams. The parameters for the simulation are as follows: the number of users $K \in \{2, 3\}$, the number of antennas $N_{\mathrm{t}} = N_{\mathrm{r}} = 64$, and the number of data streams $N_{\mathrm{s}} \in \{1, 2, 3\}$. Due to *Property 1*, the number of RF chains is set at $N_{\mathrm{t}}^{\mathrm{RF}} = N_{\mathrm{r}}^{\mathrm{RF}} = KN_{\mathrm{s}}$. We assume uniform linear arrays with antenna spacing of $\lambda/2$. The channel has $N_{\mathrm{cl}} \in \{3, 5\}$ clusters, and the number of rays is $N_{\mathrm{ray}} = 5$. The variance of the channel gains $\sigma_\alpha^2 = 1$, and the angular standard deviation (angular spread) $\sigma_{\mathrm{AS}} = 5$. In the simulation, we consider cases with both perfect and imperfect channel knowledge. For the latter, the channel estimate $\hat{\mathbf{H}}_{kj}$ is generated by $\hat{\mathbf{H}}_{kj} = \mathbf{H}_{kj} + \Delta\mathbf{H}_{kj}$, where the elements of $\Delta\mathbf{H}_{kj}$ are complex Gaussian random variables with zero mean and variance $0.1\sigma_\alpha^2$. We assume that all transmitters have the same transmit power P, and the signal-to-noise ratio (SNR) is defined as P/σ^2.

Figs. 3–5 show the average sum rate performance against SNR, where $(K, N_{\mathrm{cl}}) = (2, 3)$, $N_{\mathrm{s}} \in \{1, 3\}$ in Fig. 3 and $(K, N_{\mathrm{cl}}) = (3, 5)$,

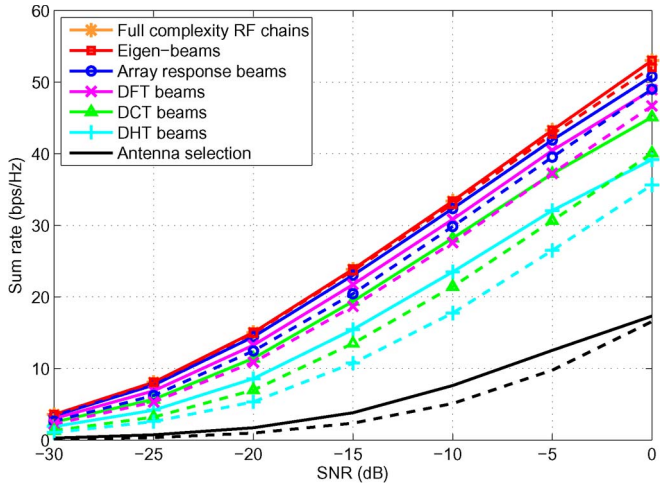

Fig. 4. Sum rate performance against SNR when $K = 3$, $N_{\rm cl} = 5$, and $N_{\rm s} = 2$. Here, the solid and dotted curves correspond to the proposed OMP-based method and the beam-steering method, respectively.

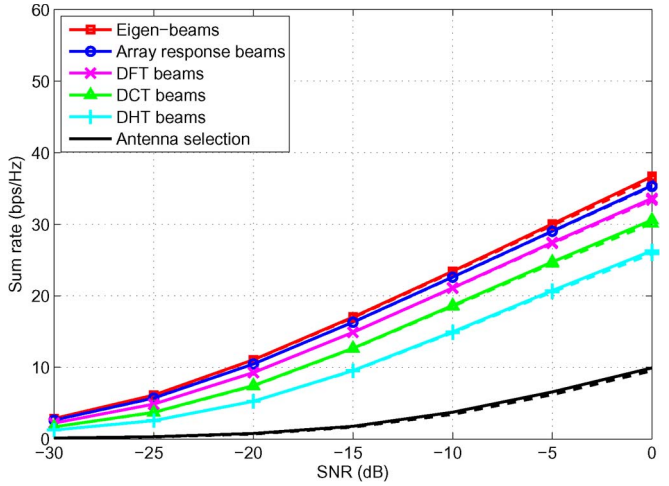

Fig. 5. Comparison between sum rates of the proposed scheme with perfect channel knowledge (solid curves) and that with channel estimates $\{\hat{\mathbf{H}}_{kj}\}$ (dash-dot curves), when $K = 2$, $N_{\rm cl} = 3$, and $N_{\rm s} = 2$.

$N_{\rm s} = 2$ in Fig. 4. For these two cases, we assume perfect channel knowledge. Channel estimation errors are considered in Fig. 5, where the simulation parameters are the same as those in Fig. 3 with the exceptions that channel knowledge is imperfect, and $N_{\rm s} = 2$. The rate curves of the proposed eigenbeamformer coincide with those of the full-complexity system because $N_{\rm t}^{\rm RF} = N_{\rm r}^{\rm RF} = KN_{\rm s}$ (*Property 1*).[3] The proposed methods outperform the beam-steering methods for all types of $\mathcal{S}_{\rm W-BF}/\mathcal{S}_{\rm F-BF}$. This happens because in the former, the RF and the baseband processors are jointly designed, whereas in the latter, they are separately designed. For the eigenbeamforming, the performance gap is small, but the gap increases for the other types of beams. Comparing the six types of beamforming vectors, as expected, the eigenbeamforming performs the best, which is followed by the array response, DFT, DCT, and DHT beamforming; the antenna selection performs the worst. It is noteworthy that the DHT beams perform reasonably well, and due to their simplicity in implementation, the use of such beams may be preferred to the phased array beams for mm-wave systems with large antenna arrays. Finally, in Fig. 5, we can see that the impact of channel estimation error on the sum rate performance is rather minor. The sum rate degradation is less than about 5% of the sum rate achieved using perfect channel knowledge for all types of beamformers.

[3]Since $N_{\rm t}^{\rm RF} = N_{\rm r}^{\rm RF} = N^{\rm RF}$, the feasibility condition in footnote 1 reduces to $N_{\rm s} \le (1/2)N^{\rm RF}$. This condition is satisfied in our simulation because $N_{\rm s} = (1/K)N^{\rm RF}$, and $K \ge 2$.

V. Conclusion

Hybrid MIMO processors for mm-wave communications over MIMO interference channels were designed by approximating the MMSE Tx/Rx processors for MIMO interference channels. Sparse approximation problems were formulated and solved by OMP-based algorithms that successively select RF beamforming vectors from a set of candidate vectors and optimize the corresponding baseband processor. We introduced six types of candidate beamforming vector sets yielding various beamformers. The proposed method jointly designs the RF beamformer and the baseband processor, and thus, it can outperform the conventional method that designs the baseband processor after steering the RF beams, as shown in the simulation. Further work in this area will include the use of other performance metrics such as max-SINR [12] for the design of hybrid MIMO systems and the application of the proposed method to hybrid MIMO systems with simplified architectures such as antenna subarrays [18].

References

[1] Z. Pi and F. Khan, "An introduction to millimeter-wave mobile broadband systems," *IEEE Commun. Mag.*, vol. 49, no. 6, pp. 101–107, Jun. 2011.
[2] T. S. Rappaport *et al.*, "Millimeter wave mobile communications for 5 G cellular: It will work!" *IEEE Access*, vol. 1, pp. 335–349, May 2013.
[3] X. Zhang, A. F. Molisch, and S. Y. Kung, "Variable-phase-shift-based RF baseband codesign for MIMO antenna selection," *IEEE Trans. Signal Process.*, vol. 53, no. 11, pp. 4091–4103, Nov. 2005.
[4] P. Karamalis, N. Skentos, and A. G. Kanatas, "Adaptive antenna subarray formation for MIMO systems," *IEEE Trans. Wireless Commun.*, vol. 5, no. 11, pp. 2977–2982, Nov. 2006.
[5] V. Venkateswaran and A. van der Veen, "Analog beamforming in MIMO communications with phase shift networks and online channel estimation," *IEEE Trans. Signal Process.*, vol. 58, no. 8, pp. 4131–4143, Aug. 2010.
[6] J. Nsenga, A. Bourdoux, W. V. Thillo, V. Ramon, and F. Horlin, "Joint Tx/Rx analog linear transformation for maximizing the capacity at 60GHz," in *Proc. IEEE Int. Conf. Commun.*, Kyoto, Japan, Jun. 2011, pp. 1–5.
[7] O. El Ayach, R. W. Heath, Jr., S. Abu-Surra, S. Rajagopal, and Z. Pi, "Low complexity precoding for large millimeter wave MIMO systems," in *Proc. IEEE Int. Conf. Commun.*, Ottawa, ON, Canada, Jun. 2012, pp. 3724–3729.
[8] A. Alkhateeb, O. El Ayach, G. Leus, and R. W. Heath, Jr., "Hybrid precoding for millimeter wave cellular systems with partial channel knowledge," in *Proc. Inf. Theory Appl. Workshop*, Feb. 2013, pp. 1–5.
[9] O. El Ayach, S. Rajagopal, S. Abu-Surra, Z. Pi, and R. W. Heath, Jr., "Spatially sparse precoding in millimeter wave MIMO systems," *IEEE Trans. Wireless Commun.*, vol. 13, no. 3, pp. 1499–1513, Mar. 2014.
[10] J. A. Tropp and S. J. Wright, "Computational methods for sparse solution of linear inverse problems," *Proc. IEEE*, vol. 98, no. 6, pp. 948–958, Jun. 2010.
[11] H. Shen, B. Li, M. Tao, and X. Wang, "MSE-based transceiver designs for the MIMO interference channel," *IEEE Trans. Wireless Commun.*, vol. 11, no. 9, pp. 3480–3489, Nov. 2010.
[12] S. W. Peters and R. W. Heath, Jr., "Cooperative algorithms for MIMO interference channels," *IEEE Trans. Veh. Technol.*, vol. 60, no. 1, pp. 206–218, Jan. 2011.
[13] T. Gou and S. A. Jafar, "Degrees of freedom of the K user $M \times N$ MIMO interference channel," *IEEE Trans. Inf. Theory*, vol. 56, no. 12, pp. 6040–6057, Dec. 2010.
[14] B. Clerckx and C. Oestges, *MIMO Wireless Networks*, 2nd ed. New York, NY, USA: Academic, 2013.
[15] A. Maltsev *et al.*, "Channel Models for 60 GHz WLAN Systems," IEEE doc. 11-09-0334-08-00ad. [Online]. Available: https://mentor.ieee.org/802.11/documents

[16] S. Yong, "TG3c Channel Modeling sub-Committee Final Report," IEEE doc. 15-07-0584-01-003c. [Online]. Available: https://mentor.ieee.org/802.15/documents
[17] J. Joung and Y. H. Lee, "Regularized channel diagonalization for multiuser MIMO downlink using a modified MMSE criterion," *IEEE Trans. Signal Process.*, vol. 55, no. 4, pp. 1573–1579, Apr. 2007.
[18] O. El Ayach, R. W. Heath, Jr., S. Rajagopal, and Z. Pi, "Multimode precoding in millimeter wave MIMO transmitters with multiple antenna sub-arrays," in *Proc. IEEE Global Telecommun. Conf.*, Atlanta, GA, USA, Dec. 2013.

The Product of Two α-μ Variates and the Composite α-μ Multipath–Shadowing Model

Elvio J. Leonardo, *Member, IEEE*, and
Michel D. Yacoub, *Member, IEEE*

***Abstract*—In this paper, the product of two independent and nonidentically distributed (i.n.i.d.) α-μ variates is considered. Exact reasonably simple closed-form expressions for the probability density function (pdf), the cumulative distribution function (cdf), and the moments of the resulting random variable (RV) are derived. These results find a wide range of applications in a number of fields, such as radar communications, multihop systems, multiple-input–multiple-input links, and cascaded communications in general. In particular, they are used here to describe a novel α-μ/α-μ composite multipath–shadowing fading model. Because the α-μ model alone comprises a substantial number of useful fading environments, its α-μ/α-μ composite version leads to a variety and an immense amount of composite fading distributions. The novel expressions for this rather flexible scenario compute instantaneously, constituting a powerful tool to characterize wireless fading channels.**

***Index Terms*—Composite fading channels, multipath fading, shadowing, α-μ distribution.**

I. Introduction

In the realm of the communication statistics, the product of random variables (RVs) arises in several opportunities and therefore is considered of great importance. For instance, high-resolution synthetic-aperture-radar clutter is modeled in [1] as the product of two fading variates. In a multihop wireless system, the random channel from a source to a destination may be obtained as the product of the RVs that describe the channel gain at each individual hop. Likewise, the cascaded fading channel, such as the one described in [2], is found as a result of the product of RVs. Moreover, such a recourse is also useful to model the keyhole channel of multiple-input–multiple-output systems [3]. Finally, composite fading statistics can be found as a special case of the statistics of the product of variates, as explored here.

The fading influencing the propagation of the radio wave is characterized by two phenomena: shadowing and multipath. Shadowing is caused by the presence of obstructions blocking the direct radio path provoking slow signal fluctuations. It is known as long-term or large-scale fading and can be observed within long distances, typically along tens or hundreds of wavelengths. Multipath is caused by reflection and scattering of the signal along the radio path provoking rapid signal fluctuations. It is known as short-term or small-scale fading and can be observed within short distances, typically along few wavelengths. The long-term fading is chiefly modeled by the lognormal distribution, although some alternate substitutes, e.g., gamma distribution, are used to circumvent the mathematical intricacy of such a model. The short-term fading is modeled by several distributions, including Rayleigh, Hoyt, Rice, Nakagami-m, Weibull, α-μ, κ-μ, and η-μ.

The separation of the combined fading into its two components, namely long term and short term, is useful not only for the physical understanding of the propagation phenomena but mainly for design purposes as well. It should, however, be applied only in approximately stationary environments. In other situations, such as vehicle-to-vehicle communications [4]–[6] and body area networks [7], [8], stationarity may be compromised, and the local mean may also fluctuate rapidly. In this sense, composite distributions, i.e., those describing the intertwined effects of both long-term and short-term fading, have been continuously raising the attention of the wireless community [9]–[19]. Those composite distributions modeling the slow fading by a lognormal process are known to render difficult analytical tractability. In fact, lognormal-based composite models do not result in closed-form expressions, and consequently, detailed analytical investigation is impaired. As stated previously, an alternative to model long-term fading is to use the gamma distribution, which approximates the lognormal distribution, yields good fitting to experimental data, and produces closed-form composite expressions [20].

In this paper, the product of two independent and nonidentically distributed (i.n.i.d.) α-μ variates is analyzed. Exact reasonably simple closed-form expressions for the probability density function (pdf), the cumulative distribution function (cdf), and the moments of the resulting RV are derived. These results are then used here to describe a novel α-μ/α-μ composite multipath–shadowing fading model. In such a model, the short-term fading is described by an α-μ distribution whose mean also follows another α-μ distribution describing the long-term fading. The resulting formulations compute instantaneously and, to the best of the authors' knowledge, are unprecedented in the literature.

The α-μ fading [21] is a general physical fading model, which considers a signal composed of clusters of multipath waves propagating in a nonhomogeneous environment. It is described by two physical fading parameters, namely α and μ, with α representing the nonlinearity of the propagation medium and μ representing the number of multipath clusters. The distribution associated with this model includes as special cases other important distributions, such as gamma (and its discrete versions Erlang and central chi-squared), Nakagami-m (and its discrete version chi), negative exponential, Weibull, one-sided Gaussian, and Rayleigh. As a result, the novel composite fading model includes as special cases a wide variety of the composite models found in the literature, such as Nakagami-m/gamma, gamma/gamma, Rayleigh/gamma, Weibull/gamma models, and others, and approximates those whose long-term fading is represented by the lognormal distribution. It is noteworthy that a two-by-two combination of the individual fading models comprised by the α-μ distribution leads to a vast variety and an immense amount of composite fading distributions. The flexibility of the α-μ distribution alone renders it adaptable to situations in which neither of the traditional distributions yields good fit [21]. In addition, its applicability has been recognized in practical scenarios. Field measurements carried out in diverse propagation environments have shown that in many situations the α-μ model better

Manuscript received September 10, 2013; revised May 21, 2014; accepted July 15, 2014. Date of publication July 23, 2014; date of current version June 16, 2015. The review of this paper was coordinated by Dr. D. W. Matolak.

E. J. Leonardo is with the Department of Informatics, State University of Maringa, 87020-900 Maringa, Brazil (e-mail: ejleonardo@uem.br).

M. D. Yacoub is with the School of Electrical and Computer Engineering, State University of Campinas, 13083-852 Campinas, Brazil (e-mail: michel@decom.fee.unicamp.br).

Digital Object Identifier 10.1109/TVT.2014.2342611